



Article

Case Study: Impact Analysis of Roof-Top Green Infrastructure on Urban System Sustainability in San José, CA

Indumathi Jeyachandran ^{1,*}  and Juneseok Lee ² ¹ Department of Civil and Environmental Engineering, San José State University, San Jose, CA 95192, USA² Department of Civil and Environmental Engineering, Manhattan University, Riverdale, NY 10471, USA; juneseok.lee@manhattan.edu

* Correspondence: indumathi.jeyachandran@sjsu.edu

Abstract: This paper presents results from a case study focusing on analyzing impacts of Green Infrastructure (GI) on sensible and latent heat fluxes, urban microclimate and the subsequent water–energy nexus components of an urban infrastructure system. The case study, focusing on the campus of a public university in San José, CA, aimed to quantify the pre- and post-conditions for a hypothetical GI implementation, which is in support of San José State University’s (SJSU) robust sustainability initiatives, which are also aligned with Silicon Valley’s broader strategic goals. The results revealed that a reduction of 0.3 °C in the average daily peak maximum temperature on campus could be achieved by the GI implementation. Air-conditioning related energy use was projected to decrease by 1.28%, monthly water use by 7052 m³, and it would result in an estimated reduction of approximately 2800 kWh in the water–energy nexus. In addition to lowering the campus’s carbon footprint, GI therefore offers significant economic and environmental benefits in terms of reductions in the urban air temperature, energy usage and water demand. This study provides valuable information for policy makers and low impact development water infrastructure managers considering GI implementation.

Keywords: Green Infrastructure (GI); latent heat; sensible heat; urban microclimate model; water–energy nexus



Citation: Jeyachandran, I.; Lee, J. Case Study: Impact Analysis of Roof-Top Green Infrastructure on Urban System Sustainability in San José, CA. *Sustainability* **2024**, *16*, 9781. <https://doi.org/10.3390/su16229781>

Academic Editor: Ali Bahadori-Jahromi

Received: 25 September 2024

Revised: 6 November 2024

Accepted: 7 November 2024

Published: 9 November 2024



Copyright: © 2024 by the authors. Licensee MDPI, Basel, Switzerland. This article is an open access article distributed under the terms and conditions of the Creative Commons Attribution (CC BY) license (<https://creativecommons.org/licenses/by/4.0/>).

1. Introduction

To counteract the negative impacts of urbanization such as flooding [1], water scarcity [2], the urban heat island (UHI) effect [3], increased energy use [4] and higher greenhouse gas (GHG) emissions [5], best management practices (BMPs) and low impact development (LID) practices are being more widely implemented in our built environment. Green roofs and porous concrete pavements are elements of what is collectively termed green infrastructure (GI), an integrated network of water infrastructure within built-up urban areas [6]. With GI now being integrated with LID concepts, the retention and detention of water in urban areas and the importation of water for supplemental irrigation has led to major changes in water budgets compared to historical approaches that were designed to expeditiously remove storm water from urban areas for flood control [7,8]. The Leadership in Energy and Environmental Design (LEED) program encourages the sustainable use of water and energy [9], and any reduction in the demand for potable water translates to energy savings and a lower carbon footprint [10]. Clearly, the two resources are closely linked, and are termed the water–energy nexus, as water is required to produce energy and energy is required to treat and transport water.

An increase in vegetated area is one option for greener and more ecologically sound city development [11]. Introducing vegetation for aesthetic reasons and to mitigate the UHI effect may slow temperature increases [3,12–15]. Increases in impervious surfaces such as parking lots hinder the creation of more vegetated spaces in urban areas. In such circumstances, vegetated or green roofs could serve as an alternative to ground level vegetated

spaces by making use of open roof surfaces. Green roofs, which involve installing vegetation on building rooftops, have become popular as a sustainable management practice for addressing various urban environmental challenges. Green roofs can significantly lower rooftop temperatures and heat amplitude, contributing to overall cooler urban temperatures and urban heat island mitigation [16–18]. Intensive green roofs, in particular, have been shown to achieve greater temperature reductions than extensive green roofs [16–18]. Green roofs help mitigate the UHI effect by lowering ambient air temperatures and improving microclimates at the neighborhood level. Additionally, the cooling effects of green roofs extend beyond the rooftops to surrounding areas, enhancing human thermal comfort and reducing heat stress [16,19].

Green roofs also reduce buildings' cooling energy demand by providing insulation and passive cooling effects. Studies report that this reduction can range from 1.3% to 50%, depending on the type of green roof and local climate. The cooling effect is particularly pronounced in hot, dry climates compared to hot, humid, or temperate climates [18,20,21]. Green roofs can also reduce the water footprint associated with energy production for cooling by lowering air conditioning energy demand, especially during peak summer months when cooling needs are high. While green roofs do consume some water directly, this is offset by the reduction in water required for energy production, resulting in an overall decrease in water use [19,22].

The objective of this paper is to present the results of a case study (in San Jose, California) to analyze the impacts of GI on latent heat fluxes, changes in the urban microclimate, the subsequent reduction in energy and water consumption as a result of temperature decreases and the consequent impact on water–energy nexus components (i.e., the reduction in energy use due to water savings).

2. Methods

In this paper, the impacts of GI on the sensible and latent heat fluxes, urban air temperature, energy and water demand and water–energy nexus in the case study site, San José State University (SJSU, San José, CA, USA) is presented.

2.1. Case Study Site

The City of San José in Northern California is the largest city in Silicon Valley, the third largest city in the state and the tenth largest city in the US. The main campus of San José State University (SJSU), which is located in downtown San José, extends over 154 acres and supports about 32,500 undergraduate and graduate students, of whom about 3500 live on campus. The main campus consists of about 43 buildings, including classrooms, dormitories, science labs, athletic facilities, kitchens and cafeterias. San José's wet season runs from October to February; summer in San José has near zero precipitation, so huge irrigation is required at this time of year.

With SJSU's strong sustainability initiatives/activities, this study aims to study the impact of GI implementation, which potentially consists of installing irrigated green roofs on nearly 98% of the campus rooftops, with the sole exception of parking garages (Figure 1). As SJSU has a very dense footprint, primarily consisting of buildings with only a very limited amount of open parking lots, only green rooftops were considered in this study. The type of green roofs which were used for this study are intensive green roofs, which require a deeper growing medium and can accommodate larger plants, which have implications in terms of enhanced stormwater management, increased carbon sequestration, improved air quality, as well as improved thermal insulation [23]. As noted in the previous section, this study aims to assess the specific impacts of green infrastructure (GI) on sensible and urban heat fluxes, the urban microclimate, energy demand, water demand and the water–energy nexus components at the SJSU main campus. These insights are intended to support university administrators in their implementation decision-making.

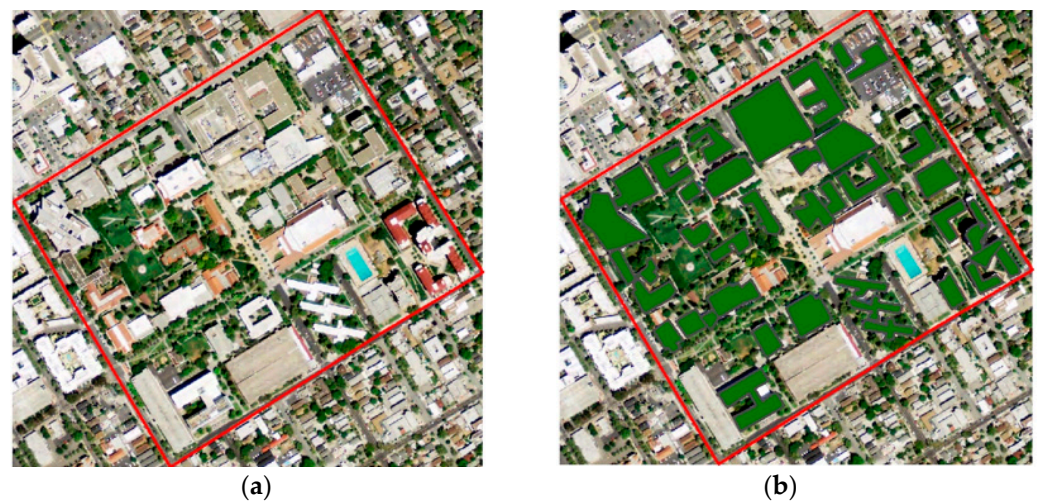


Figure 1. SJSU is having a significant campus-wide sustainability initiative. The figures show the (a) selected case study area before and (b) after the hypothetical green infrastructure implementation.

2.2. Modeling Methodology

The modeling framework used to study the impacts of green infrastructure consists of five sub-models that individually simulate (i) urban heat fluxes, (ii) urban microclimate, (iii) energy demand changes, (iv) water demand changes and (v) water–energy nexus components. The following data sources are used: (i) remote sensing data for generating surface resistance maps and aerial photos of the study area obtained from National Map Viewer, (ii) meteorological tower measurements of temperature, relative humidity, albedo and wind speed for heat flux modeling, provided by the National Climatic Data Center (NCDC, Asheville, NC, USA), and (iii) water demand data were provided by the local office of Facilities Development and Operation, as was (iv) the corresponding pump station energy use data. The procedures performed included: (i) pre-processing the remote sensing data; (ii) building and running appropriate coding to compute the heat fluxes and ET, calculating temperature changes using an urban heat flux model and a microclimate model; and (iii) feeding the temperature and ET values into the sub-models to compute energy and water demand changes and model the water–energy nexus (Figure 2). Details of each sub-model are explained in turn below.

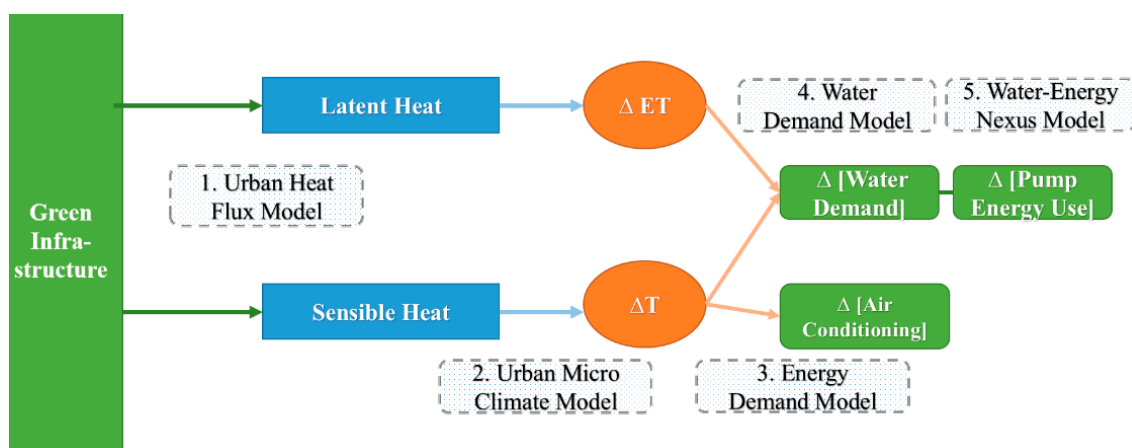


Figure 2. Framework of the models used for this case study.

2.2.1. Urban Heat Flux Model

The urban heat flux model (UHFL) developed by Jeyachandran [24] is a modified version of the Local-scale Urban Meteorological Parameterization Scheme (LUMPS) model [25]

which computes sensible and latent heat fluxes. Sensible and latent heat fluxes are part of the Surface Energy Balance (SEB). The SEB for urban areas is given as:

$$R_n = Q_H + Q_E + \Delta Q_S \quad (1)$$

The net radiation (R_n) at the surface is partitioned into the sensible heat flux, latent heat flux, and storage heat flux. In urban areas, the ground heat flux on a daily time scale is considered negligible [25]. The sensible heat flux (Q_H) is associated with temperature change and arises as a result of the difference in temperatures of the surface and the air above. The latent heat flux (Q_E) is a result of cooling associated with a phase change and with mass transfer from the surface (e.g., water vapor). The storage heat flux (ΔQ_S) is a residual of the difference between net radiation and sensible and latent heat fluxes. The sensible and latent heat fluxes serve as key boundary conditions for weather forecast models [26] and they also play a major role in controlling the urban microclimate.

In the UHFL [24], the parameterizations for the sensible and latent heat fluxes follow those used in LUMPS, except for the new parameters α_{new} and β_{new} [25] that are applied:

$$Q_E = \alpha_{new} \left(\frac{\Delta}{(\Delta + \gamma)} \right) (R_n - \Delta Q_S) + \beta_{new} \quad (2)$$

$$Q_H = \left[\left(\frac{(1 - \alpha_{new}) \Delta + \gamma}{\Delta} + \gamma \right) (R_n - \Delta Q_S) - \beta_{new} \right] \quad (3)$$

where Q_E is the latent heat flux ($W m^{-2}$), Q_H is the sensible heat flux ($W m^{-2}$), R_n is the net radiation ($W m^{-2}$), ΔQ_S is the storage heat flux ($W m^{-2}$), Δ is the slope of the saturation vapor pressure versus temperature curve ($kPa \text{ } ^\circ C^{-1}$) and γ is the psychrometric constant ($kPa \text{ } ^\circ C^{-1}$). The parameters α_{new} and β_{new} are estimated from the two multivariable regression equations below by using inputs of soil moisture, surface cover properties (surface resistance and aerodynamic resistance), temperature, relative humidity and vapor pressure deficit (Equations (3) and (4)), explained in greater detail in Section 2.2.7:

$$\alpha_{new} = -1.74 - 0.05 \times \delta_e + 0.01 \times w\%(IR) - 0.43 \times w\%(NIR) - 0.03 \times r_s(IR) + 0.03 \times r_s(NIR) \quad (4)$$

$$\beta_{new} = -80.77 + 0.13 \times T - 0.68 \times r_s(IR) + 0.64 \times r_s(NIR) + 0.15 \times RH - 0.03 \times r_a \quad (5)$$

where δ_e is the vapor pressure deficit (kPa), $w\%(IR)$ is the soil moisture content at irrigated sites (%), $w\%(NIR)$ is the soil moisture content at non-irrigated sites (%), $r_s(IR)$ is the surface resistance at irrigated sites and $r_s(NIR)$ is the surface resistance at non-irrigated sites, T is the air temperature ($^\circ C$), $r_s(IR)$ is the surface resistance at irrigated sites, $r_s(NIR)$ is the surface resistance at non-irrigated sites, RH is the relative humidity, and r_a is the aerodynamic resistance.

As in LUMPS [25], the Objective Hysteresis Model [27] is used to model the storage heat flux (ΔQ_S), and is given as:

$$\Delta Q_S = \sum_{i=1}^n (f_i a_{1i}) \cdot R_n + \sum_{i=1}^n (f_i a_{2i}) \cdot \frac{\partial R_n}{\partial t} + \sum_{i=1}^n (f_i a_{3i}) \quad (6)$$

where R_n is the net radiation, f is the fraction of surface cover types and a_1 , a_2 and a_3 are the corresponding coefficients [25].

Sensitivity analysis was performed for the parameters α_{new} and β_{new} in the study by Jeyachandran [24]. It was found out that the most dominant factor influencing α_{new} is the surface resistance at irrigated sites, followed by vapor pressure deficit and soil moisture at irrigated sites. For β_{new} , surface resistance at irrigated sites, followed by relative humidity, temperature and aerodynamic resistance turned out to be the most influential factors. As the surface resistance decreases, the value of β_{new} increases, which in turn results in an increase in latent heat flux and an increase in sensible heat flux [24].

The time step used for modeling sensible and latent heat flux was 30 min. The urban heat flux model is highly sensitive to changes in surface resistance, vapor pressure deficit and soil moisture, as evidenced in the study by Jeyachandran [24].

2.2.2. Urban Microclimate Model

The effect of sensible heat flux on air temperature is modeled using the one-dimensional model proposed by Oke [28] and Cleugh et al. [29]:

$$\frac{dT_a}{dt} = \frac{Q_H}{Z_{UBL}} \quad (7)$$

where $\frac{dT_a}{dt}$ is the diurnal heating rate ($^{\circ}\text{C s}^{-1}$), Q_H is the sensible heat flux in kinematic units (also referred as H) ($\text{ms}^{-1} \text{ }^{\circ}\text{C}$) and Z_{UBL} is the depth of the boundary layer (assumed to be 1 km), The sensible heat flux (Q_H) predicted by the urban heat flux model [24] is converted to sensible heat flux in kinematic units (H) for use in the urban microclimate model:

$$H = \frac{Q_H}{(\rho \times c_p)} \quad (8)$$

where H is the sensible heat flux in kinematic units ($\text{ms}^{-1} \text{ }^{\circ}\text{C}$), Q_H is the sensible heat flux (W m^{-2}), ρ is the density of air (1.22 kg/m^{-3}) and c_p is the specific heat of air ($1.013 \times 10^3 \text{ Jkg}^{-1} \text{ }^{\circ}\text{C}^{-1}$). The diurnal heating rate (dT_a/dt) ($^{\circ}\text{Ch}^{-1}$) is used to predict the peak afternoon summertime temperature ($^{\circ}\text{C}$). Although this one-dimensional model does not account for mesoscale advection, it is known to be useful for first-order studies of the heat flux–microclimate interrelationship [29,30].

2.2.3. Energy Demand Model

The model used to compute peak maximum energy demand (E_{max} in MWh) requires an input of Cooling Degree Days (CDD), with $65 \text{ }^{\circ}\text{F}$ as the base temperature for calculating CDD , as stated in Jeyachandran [24]:

$$E_{max} = 1.517 \times CDD + 38.934 \quad (9)$$

For instance, if CDD is 25, then E_{max} as per Equation (9) is 76.86 MWh.

2.2.4. Water Demand Model

Renwick and Green [31] formulated and estimated an econometric model for residential water demand. Their analysis relies on cross-sectional monthly time-series data for eight water agencies in California, representing 24% of the state's population. The water demand equation is specified in a logarithmic functional form and the model captures the influence of variation in climate as one of the independent variables, with changes in water demand as a dependent variable (Equation (10)).

$$\ln W_{it} = \beta_0 + \beta_1 \ln(TEMP)_{it} + \dots + e_{it} \quad (10)$$

where W_{it} is the average monthly water use in CCF (Hundred Cubic Feet; $1 \text{ CCF} = 2.83 \text{ m}^3$); $TEMP$ is the deviation of temperature from normal patterns; and e_{it} refers to the residuals.

This econometric model explicitly incorporates a harmonic model to separately capture the effects of seasonality and climatic variability on demand. The climatic variables represent only the effect of deviations of the climate from normal patterns in the demand equation. The variables considered in the model include marginal price, income, lot size, and other demand-side management strategies. For our purposes, other variables are assumed to remain constant and only temperature changes, allowing us to focus on capturing water demand changes. The coefficient for $\ln TEMP$ (temperature in degrees Fahrenheit; average maximum daily air temperature) was found to be 0.45 (statistically significant at

the 0.01 level), indicating that higher-than-average maximum daily air temperatures will increase the water demand.

2.2.5. Water–Energy Nexus

The main campus well, positioned 91 feet above sea level, services all 43 buildings and the central plant within a unified pressure zone. Located in the campus’s southeast quadrant (Figure 1), it has operated since at least 1940, with a variable frequency drive pump in use for the past 24 years. To evaluate water and energy metrics, data from meters tracking usage are collected monthly; water consumption data goes back to January 2001, and energy data to November 2006. Isolated from external influences, this setup supports pure demand monitoring and analysis. In this vein, the relationship between water demand and pump energy use can be used, which underscores the close linkage between water and energy. We therefore utilized water use vs. pump energy data to calculate the corresponding energy use reduction due to water savings.

2.2.6. Total Carbon Equivalence

In the previous sections, water and energy savings were calculated. Based on these energy values, the carbon equivalence for the amount of energy produced is calculated following the EPA’s equivalence factor 6.89551×10^{-4} metric tons CO₂/kWh [32]. The sum of the air conditioning and pump energy impacts can now be calculated in terms of the total carbon equivalence.

2.2.7. Urban Heat Flux and Microclimate Model Parameters

For the first step, the urban heat flux model was run for three rainless summer days in July 2014, 17 July to 19 July, with a 30 min time step. The meteorological data needed for the heat flux model was obtained from the National Climatic Data Center (NCDC). The meteorological data and two other important parameters, surface resistance (r_s) and soil moisture (w%), play a vital role in the partitioning of the net radiation (R_n) into sensible and latent heat fluxes (Q_H and Q_E). The urban heat flux model was used to simulate the sensible and latent heat flux for both the pre- and post-GI implementation scenarios. The input parameters used to compute the α_{new} and β_{new} parameters were varied as shown in Table 1 to reflect the implementation of GI, considering the effect of the urban landscape, soil moisture, surface characteristics (surface resistance and aerodynamic resistance) and meteorological factors (vapor pressure deficit, temperature and wind speed) to estimate surface energy fluxes.

Table 1. Model parameters for pre- and post-GI implementation.

Model Parameter	Pre-GI	Post-GI	Source
Soil moisture (%)	2	20	Field measurements
Surface resistance (s m ⁻¹)	70	55	Surface resistance map

In order to represent the modified surface characteristics corresponding to the pre-GI and Post-GI conditions, the soil moisture (w%) and surface resistance (r_s) values used to estimate α_{new} and β_{new} parameters used in the model were selected accordingly. As the soil moisture conditions in intensive green roofs after irrigation are assumed to be the same across the US, the soil moisture and surface resistance values used were taken from a previous case study [33]. The average surface resistance value for the pre-GI scenario (Table 1) was based on a surface resistance map created by using a Leaf Area Index map to compute surface resistance utilizing the formula described by Allen et al. [34]. The LAI map was based on a normalized difference vegetation index (NDVI) map generated from Landsat data for the month of July, following the method proposed by Yin and Williams [35]. Both the LAI map and the surface resistance map were created in Esri’s ArcMap using raster calculator tools. In both the LAI for the Post-GI scenario, the surface resistance value

for an existing green roof was used and the green roofs were assumed to be water intensive, thus requiring irrigation (Table 1).

The sensible heat flux output from the urban heat flux model is fed into the urban microclimate model [28] to compute the peak maximum afternoon temperature and diurnal heating as shown in Equations (5) and (6).

3. Results and Discussion

3.1. Urban Heat Fluxes

The input parameters used to compute α_{new} and β_{new} in the urban heat flux model were changed to reflect the pre-GI and post-GI conditions and both the surface resistance (r_s) and soil moisture (w%) were varied to characterize these scenarios as stated in Table 1. The simulated heat fluxes for the two scenarios are shown in Figures 3–5, which show the data for July 17th, 18th and 19th, 2014, respectively. As expected, the post-GI scenarios exhibit higher latent heat flux than the pre-GI scenarios as a result of the hypothesized GI implementation, which contributes to the cooling of the urban environment. Latent heat flux contributes to the cooling of the atmosphere, and with lesser latent heat flux (evapotranspiration) there is a greater amount of partitioning of the net radiation into sensible heat flux, which in turn contributes to an increase in urban air temperature.

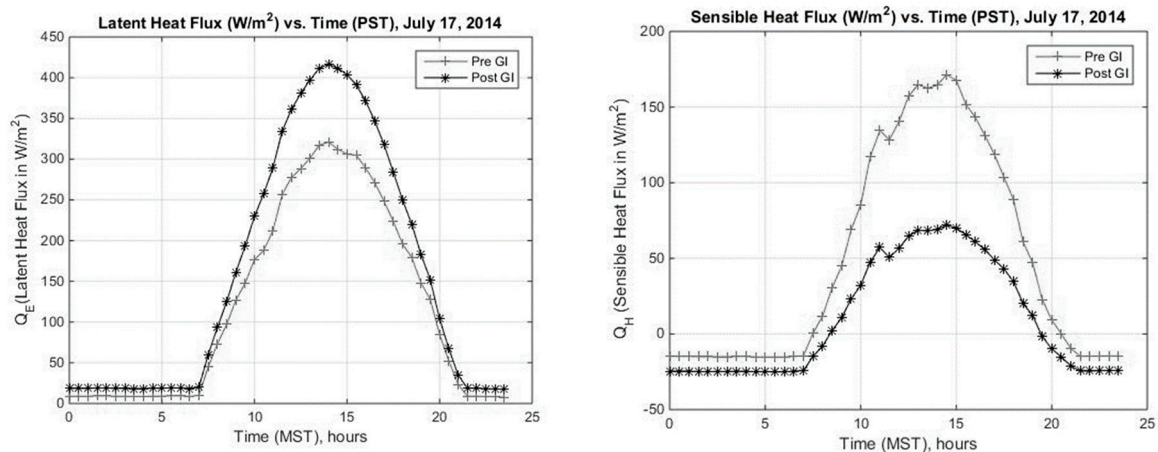


Figure 3. Comparison of simulated 17 July 2014 latent and sensible heat fluxes for pre-GI and post-GI conditions on the campus of San José State University.

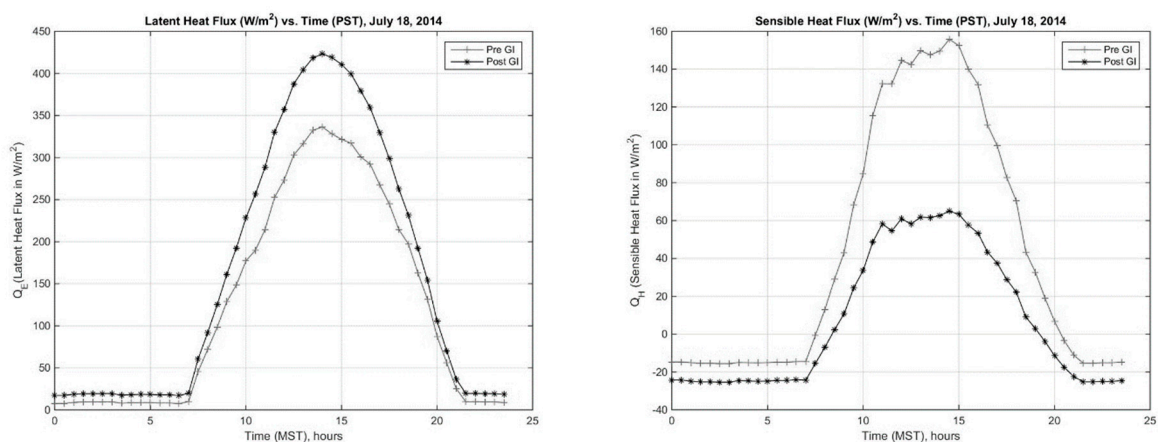


Figure 4. Comparison of simulated 18 July 2014 latent and sensible heat fluxes for pre-GI and post-GI conditions on the campus of San José State University.

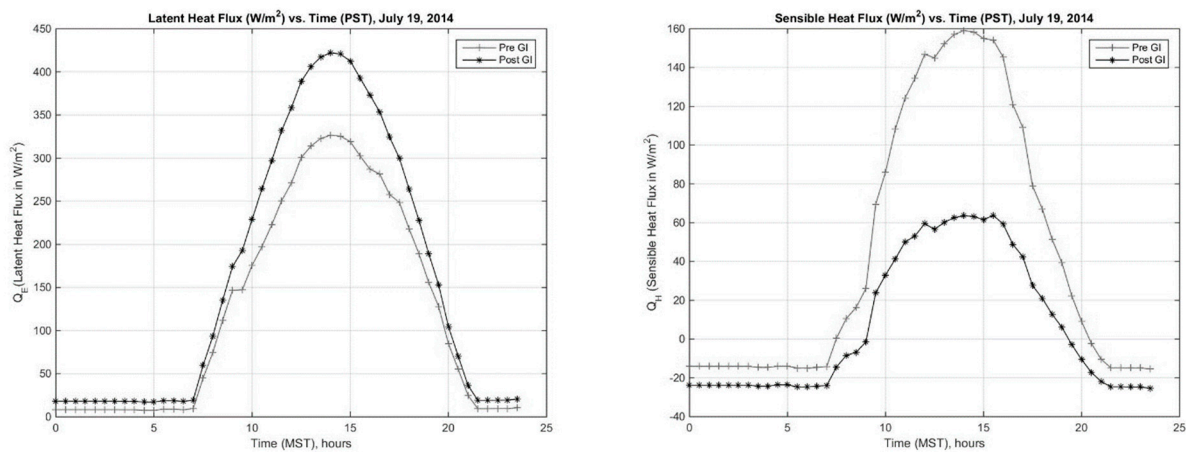


Figure 5. Comparison of simulated 19 July 2014 latent and sensible heat fluxes for pre-GI and post-GI conditions on the campus of San José State University.

3.2. Urban Microclimate

The midday sensible heat flux at 1 pm is used as an input to the boundary layer climate model by Oke [28] (Equation (7)) to simulate the diurnal heating rate (dT_a/dt), which is then used to compute the summertime daily maximum air temperature. The diurnal heating rate in the pre-GI scenario is higher than the post-GI scenario by an average of around 0.3 °C, which can be inferred from Table 2.

Table 2. Effect on peak afternoon air temperature for the two scenarios.

Date	Diurnal Heating Rate	Diurnal Heating Rate
	(°Ch ⁻¹) <i>Pre-GI</i>	(°Ch ⁻¹) <i>Post-GI</i>
17 July 2014	0.48	0.19
18 July 2014	0.43	0.18
19 July 2014	0.44	0.17
Average	0.45	0.18
Std. dev.	0.03	0.01

The high relative humidity in California contributes to the low vapor pressure deficit (VPD) and, consequently, an increase in α_{new} , which in turn increases the latent heat flux. This corresponds with the phenomenon established by Nemani and Running [36], who concluded that low VPD and good soil moisture, along with low surface resistance and low aerodynamic resistance, contribute to an increase in latent heat flux. The peak maximum latent heat flux for the Pre-GI and Post-GI scenarios shown in Table 3 reveals a significant difference in the peak maximum latent heat flux values for the two scenarios, corresponding to an average of 92 W m⁻².

Table 3. Change in peak latent heat flux (ET) achieved by GI.

Date	Latent Heat Flux	Latent Heat Flux	Increase in Latent Heat Flux (W m ⁻²)
	(W m ⁻²) <i>Pre-GI</i>	(W m ⁻²) <i>Post-GI</i>	
17 July 2014	302	397	95
18 July 2014	317	405	88
19 July 2014	314	406	92
Average	311	403	92
Std. dev.	7.93	4.93	3.51

3.3. Energy Demand

The peak maximum daily air temperatures for the two scenarios were calculated from the diurnal heating rate in Table 2. The peak maximum daily air temperature was then used to compute CDD and was fed into Equation (7) to compute the peak maximum daily energy usage.

The peak maximum energy usage results indicate that the average temperature difference of nearly 0.3 °C (Table 2) between the pre-GI and post-GI scenarios would lead to an average reduction in energy usage of 1.28% (Table 4). This result is similar to the results of a study by Akbari et al. [4], who analyzed five cities in the US (Los Angeles, Washington DC, Phoenix, Tucson and Colorado Springs) and found an increase of 2% to 4% in energy usage for every 1 °C rise in daily maximum temperature above a base temperature of 15 to 20 °C.

Table 4. Change in Peak Maximum Energy Use achieved by GI (total energy use for SJSU).

Date	Peak maximum Energy Usage (kWh) <i>Pre-GI</i>	Peak Maximum Energy Usage (kWh) <i>Post-GI</i>	Difference in Energy Usage	Percentage Decrease in Energy Usage (%)
17 July 2014	58,500	57,600	900	1.53
18 July 2014	55,200	54,600	600	1.08
19 July 2014	58,300	57,600	700	1.20
Average	57,333	56,600	733	1.27
Std. dev.	1850.22	1732.05	153	0.23

3.4. Water Demand

An average daily peak maximum temperature reduction of 0.3 °C will also reduce the water demand on campus. Given a high temperature of 29.4 °C (85 °F) and an average temperature of 16.7 °C (62 °F) in Equation (8) and considering the number of residents (about 3500) in Campus Village during the summertime, the reduction in the total water demand is estimated to be 7052 m³ (2482 CCF).

3.5. The Water–Energy Nexus

Figure 6 illustrates the water–energy nexus by plotting water withdrawal against energy consumption, revealing a linear relationship between water demand and pump energy usage. According to SJSU’s water–energy relationship (Figure 6), a reduction of 7052 m³ in the campus water usage will correspond to a reduction of about 2800 kWh in energy consumption.

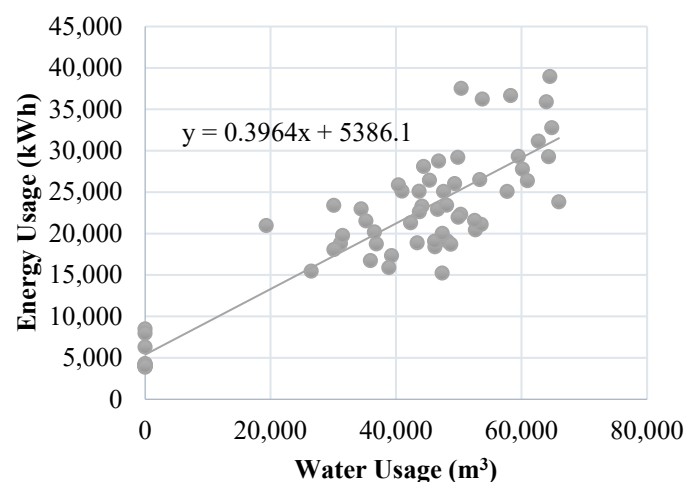


Figure 6. Water Usage versus Energy Usage in SJSU.

3.6. Total Carbon Footprint

Following EPA's equivalence factor, 6.89551×10^{-4} metric tons CO₂/kWh, the water–energy nexus will reduce the campus's carbon footprint by about 2 metric tons of CO₂.

3.7. Discussion

The modeling study provided valuable insights on potential impacts on sensible and latent heat fluxes, urban air temperature, energy usage, water use and the water–energy nexus by the hypothetical implementation of GI in the SJSU. Following the implementation of GI, the average increase in latent heat flux was found to be 92 W m^{-2} . The increase in latent heat flux contributes to a reduction in the peak maximum air temperature. A reduction of $0.3 \text{ }^\circ\text{C}$ in the campus' average daily peak maximum temperature due to GI implementation was calculated. This reduction not only supports sustainability goals but also has practical implications for enhancing comfort and air quality on campus.

Furthermore, the study found the average temperature difference between the pre-GI and post-GI scenarios would correspond to an average reduction in energy usage by 1.28%, primarily due to air-conditioning. The corresponding reduction in monthly water use was found to be about 7052 m^3 , saving about 2800 kWh of electricity at the pump station. Collectively, these findings translate to a total reduction of 2 metric tons of CO₂ emissions from the pump station alone.

The implementation of GI carries broader benefits for the community, including reducing the adverse effects of heat waves on human health [37] and lowering urban air particulate pollution [38]. However, cost is an essential factor to consider, as green roofs can range from USD 15 to USD 50 per square foot, with maintenance costs varying depending on whether the roof is intensive or extensive. Therefore, while the benefits of GI are clear from this study and many others, the economic viability as well as funding sources for implementation must be assessed carefully.

It is important to note the robustness of the modeling approach presented in this paper, which incorporates realistic assumptions regarding GI effectiveness in a highly urban environment in California. Also, the integration of water–energy nexus analysis within the GI assessment framework is an innovative aspect of the study, enabling a comprehensive evaluation of how these systems function. However, there are limitations that require attention. The study's findings are based on a hypothetical scenario for a single University campus, which may limit the generalization of the results to other urban areas with different layouts, climate characteristics or infrastructure. Also, there are potential limitations related to modeling assumptions, such as seasonal variations in GIS effectiveness or specific climate controls, as these factors/parameters may impact the accuracy of the findings.

4. Conclusions

This paper presents findings from a case study analyzing the impacts of GI on sensible and latent heat fluxes, the urban microclimate, and resulting energy and water savings within the water–energy nexus of an urban infrastructure system. The main campus of SJSU in San Jose, California, served as the study site. Results indicate that implementing GI on the SJSU campus would offer substantial economic and environmental benefits, including lower urban air temperatures, reduced energy usage, decreased water demand, and minimized carbon footprint.

Beyond the SJSU campus, these findings underscore the broader potential for urbanized cities worldwide to adopt GI as a viable strategy for enhancing urban resilience, mitigating heat effects, and achieving significant water–energy savings. Future research could focus on validating these findings across diverse urban environments, examining site-specific variables, and developing optimization models for GI planning to maximize benefits in areas with varied climates and infrastructure layouts. The insights from this study offer valuable guidance for cities and planners aiming to integrate sustainable infrastructure solutions to address urban climate challenges and sustainable resource management.

Author Contributions: I.J. and J.L. contributed to the following: study conception and design, data collection, analysis and interpretation of results, and manuscript preparation. All authors have read and agreed to the published version of the manuscript.

Funding: This research received no external funding.

Institutional Review Board Statement: Not applicable.

Informed Consent Statement: Not applicable.

Data Availability Statement: The datasets generated during and/or analyzed during the current study are available from the corresponding author on reasonable request.

Conflicts of Interest: The authors declare no conflicts of interest.

References

- Hollis, G.E. The effect of urbanization on floods of different recurrence interval. *Water Resour. Res.* **1975**, *11*, 431–435. [CrossRef]
- Postel, S.L. Entering an era of water scarcity: The challenges ahead. *Ecol. Appl.* **2000**, *10*, 941–948. [CrossRef]
- Rosenfeld, A.H.; Akbari, H.; Romm, J.J.; Pomerantz, M. Cool communities: Strategies for heat island mitigation and smog reduction. *Energy Build.* **1998**, *28*, 51–62. [CrossRef]
- Akbari, H.; Pomerantz, M.; Taha, H. Cool surfaces and shade trees to reduce energy use and improve air quality in urban areas. *Sol. Energy* **2001**, *70*, 295–310. [CrossRef]
- Pataki, D.E.; Alig, R.J.; Fung, A.S.; Golubiewski, N.E.; Kennedy, C.A.; McPherson, E.G.; Nowak, D.J.; Pouyat, R.V.; Romero Lankao, P. Urban ecosystems and the North American carbon cycle. *Glob. Change Biol.* **2006**, *12*, 2092–2102. [CrossRef]
- Benedict, M.; McMahon, E. Green infrastructure, 2002: Smart conservation for the 21st century. *Renew. Resour. J.* **2002**, *20*, 12–17.
- Lee, J.; Younos, T.; Parece, T.E. Decentralized Green Water-Infrastructure Systems: Resilient and Sustainable Management Strategies for Building Water Systems. In *Resilient Water Management Strategies in Urban Settings: Innovations in Decentralized Water Infrastructure Systems*; Springer International Publishing: Cham, Switzerland, 2022; pp. 1–20.
- Younos, T.; Lee, J.; Parece, T. Twenty-first century urban water management: The imperative for holistic and cross-disciplinary approach. *J. Environ. Stud. Sci.* **2019**, *9*, 90–95. [CrossRef]
- USGBC. LEED. 2015. Available online: <http://www.usgbc.org/leed> (accessed on 25 September 2024).
- Lee, J.; Younos, T. Sustainability Strategies at the Water–Energy Nexus. *J. AWWA* **2018**, *110*, 32–39. [CrossRef]
- Dunnett, N.; Kingsbury, N. Planting Options for Extensive and Semi-Extensive Green Roofs. In Proceedings of the 2nd Annual International Greening Rooftops for Sustainable Communities Conference, Awards and Trade Show, Portland, OR, USA, 2–4 June 2004.
- Grimmond, C.S.; Souch, C.; Hubble, M.D. Influence of tree cover on summertime surface energy balance fluxes, San Gabriel Valley, Los Angeles. *Clim. Res.* **1996**, *6*, 45–57. [CrossRef]
- Bonan, G.B. The microclimates of a suburban Colorado (USA) landscape and implications for planning and design. *Landsc. Urban Plan.* **2000**, *49*, 97–114. [CrossRef]
- Dimoudi, A.; Nikolopoulou, M. Vegetation in the urban environment: Microclimatic analysis and benefits. *Energy Build.* **2003**, *35*, 69–76. [CrossRef]
- Kottmeier, C.; Biegert, C.; Corsmeier, U. Effects of urban land use on surface temperature in Berlin: Case study. *J. Urban Plan. Dev.* **2007**, *133*, 128–137. [CrossRef]
- Peng, L.L.; Jim, C.Y. Green-roof effects on neighborhood microclimate and human thermal sensation. *Energies* **2013**, *6*, 598–618. [CrossRef]
- Aboelata, A. Assessment of green roof benefits on buildings’ energy-saving by cooling outdoor spaces in different urban densities in arid cities. *Energy* **2021**, *219*, 119514. [CrossRef]
- Morakinyo, T.E.; Dahanayake, K.K.; Ng, E.; Chow, C.L. Temperature and cooling demand reduction by green-roof types in different climates and urban densities: A co-simulation parametric study. *Energy Build.* **2017**, *45*, 226–237. [CrossRef]
- Hirano, Y.; Ihara, T.; Gomi, K.; Fujita, T. Simulation-based evaluation of the effect of green roofs in office building districts on mitigating the urban heat island effect and reducing CO₂ emissions. *Sustainability* **2019**, *11*, 2055. [CrossRef]
- Jaffal, I.; Ouldboukhite, S.E.; Belarbi, R. A comprehensive study of the impact of green roofs on building energy performance. *Renew. Energy* **2012**, *43*, 157–164. [CrossRef]
- Cirrincone, L.; Marvuglia, A.; Scaccianoce, G. Assessing the effectiveness of green roofs in enhancing the energy and indoor comfort resilience of urban buildings to climate change: Methodology proposal and application. *Build. Environ.* **2021**, *205*, 108198. [CrossRef]
- Pirouz, B.; Palermo, S.A.; Maiolo, M.; Arcuri, N.; Piro, P. Decreasing water footprint of electricity and heat by extensive green roofs: Case of southern Italy. *Sustainability* **2020**, *12*, 10178. [CrossRef]
- Berardi, U.; GhaffarianHoseini, A.; GhaffarianHoseini, A. State-of-the-art analysis of the environmental benefits of green roofs. *Appl. Energy* **2014**, *115*, 411–428. [CrossRef]

24. Jeyachandran, I. Effects of Landscape Modification on Evapotranspiration, Microclimate, Energy Use, and Water Use in Urban Environments. Ph.D. Thesis, Department of Civil and Environmental Engineering, University of Utah, Salt Lake City, UT, USA, 2009; p. 127.
25. Grimmond, C.S.; Oke, T.R. Turbulent heat fluxes in urban areas: Observations and a local-scale urban meteorological parameterization scheme (LUMPS). *J. Appl. Meteorol. Climatol.* **2002**, *41*, 792–810. [[CrossRef](#)]
26. Holtslag, A.A.; Van Ulden, A.P. A simple scheme for daytime estimates of the surface fluxes from routine weather data. *J. Appl. Meteorol. Climatol.* **1983**, *22*, 517–529. [[CrossRef](#)]
27. Grimmond, C.S.; Cleugh, H.A.; Oke, T.R. An objective urban heat storage model and its comparison with other schemes. *Atmos. Environ.* **1991**, *25*, 311–326. [[CrossRef](#)]
28. Oke, T. The micrometeorology of the urban forest. *Philos. Trans. R. Soc.* **1989**, *324*, 335–351.
29. Cleugh, H.A.; Bui, E.; Simon, D.; Xu, J.; Mitchell, V.G. The Impact of Suburban Design on Water Use and Microclimate. In Proceedings of the MODSIM 2005 International Congress on Modelling and Simulation, Melbourne, Australia, 12–15 December 2005; pp. 10–14.
30. Mitchell, V.G.; Cleugh, H.A.; Grimmond, C.S.; Xu, J. Linking urban water balance and energy balance models to analyse urban design options. *Hydrol. Process. Int. J.* **2008**, *22*, 2891–2900. [[CrossRef](#)]
31. Renwick, M.E.; Green, R.D. Do residential water demand side management policies measure up? An analysis of eight California water agencies. *J. Environ. Econ. Manag.* **2000**, *40*, 37–55. [[CrossRef](#)]
32. EPA. Clean Energy. Calculations and References. 2015. Available online: <https://www.nrc.gov/docs/ML1320/ML13205A377.pdf> (accessed on 25 September 2024).
33. Jeyachandran, I.; Burian, S.J.; Pardyjak, E.R.; Pomeroy, C.A.; Skousen, B. Impact of green infrastructure on urban energy fluxes and microclimate. In Proceedings of the EWRI 2010 International Conference on Water Resources and the Environment, Chennai, India, 5–7 January 2010.
34. Allen, R.G.; Jensen, M.E.; Wright, J.L.; Burman, R.D. Remote sensing surface energy balance algorithm for land (SEBAL). 1. Formulation. *J. Hydrol.* **1989**, *81*, 650–662.
35. Yin, Z.; Williams, T.L. Obtaining spatial and temporal vegetation data from Landsat MSS and AVHRR/NOAA satellite images for a hydrologic model. *Photogramm. Eng. Remote Sens.* **1997**, *63*, 69–77.
36. Nemani, R.R.; Running, S.W. Estimation of regional surface resistance to evapotranspiration from NDVI and thermal-IR AVHRR data. *J. Appl. Meteorol. Climatol.* **1989**, *28*, 276–284. [[CrossRef](#)]
37. Marvuglia, A.; Koppelaar, R.; Rugani, B. The effect of green roofs on the reduction of mortality due to heatwaves: Results from the application of a spatial microsimulation model to four European cities. *Ecol. Model.* **2020**, *438*, 109351. [[CrossRef](#)]
38. Speak, A.F.; Rothwell, J.J.; Lindley, S.J.; Smith, C.L. Urban particulate pollution reduction by four species of green roof vegetation in a UK city. *Atmos. Environ.* **2012**, *61*, 283–293. [[CrossRef](#)]

Disclaimer/Publisher’s Note: The statements, opinions and data contained in all publications are solely those of the individual author(s) and contributor(s) and not of MDPI and/or the editor(s). MDPI and/or the editor(s) disclaim responsibility for any injury to people or property resulting from any ideas, methods, instructions or products referred to in the content.